WARSAW UNIVERSITY OF TECHNOLOGY Index 351733
FACULTY OF CIVIL ENGINEERING
COMMITTEE FOR CIVIL AND WATER ENGINEERING
POLISH ACADEMY OF SCIENCES ISSN 1230-2945
DOI: 10.24425/ace.2025.156174
ARCHIVES OF CIVIL ENGINEERING
Vol. LXXI ISSUE 4 2025
pp. 343 –358

Research paper

Research on construction control of long-linked continuous beam bridge closure

Xilong Zheng[1]

Abstract: In this paper, four feasible closing schemes are proposed, three of which are optimization schemes, and the deformation and internal force of the main beam are taken as the control elements, and the closing conditions, cumulative vertical displacement, lower and lower edge stress on the cross-section and horizontal displacement of the support are compared and analysed under different closure sequence schemes. It is found that the displacement and stress differences are large in different closure sequence schemes, different structural system conversion timings, and it is necessary to carry out optimization studies and comprehensively compare and select reasonable schemes. The construction control of the closure stage is studied, and the results of bridge construction control are compared, which shows that the optimization technology and construction control technology of the closure sequence can be used in this paper, which can solve the key problems in the construction control of the closure of long-link continuous beam bridges, and can provide reference and basis for the construction control of the same type of bridge.

Keywords: long-linked continuous beam bridge, construction control, closure scheme, solution optimization

[1]PhD., Harbin University, School of Civil and Architectural Engineering, No.109 Zhongxing Da Dao, Harbin, China
e-mail: sampson88@126.com, ORCID: 0000-0001-5571-667X

1. Background

The selection of the closure sequence and the construction quality of the closure section are related to the rationality of the bridge state and have a huge impact on the safety of the bridge in the operation stage [1–3]. First of all, the number of super static determination of the long-linked continuous beam bridge is high, and the system conversion, temperature change, prestressed beam tension and concrete shrinkage creep in the construction of the closure will produce a large internal force or sub-internal force redistribution, which has an impact on the displacement and internal force state of the structure in the whole construction stage [4–8]. The construction of the closure is a difficult point in the construction of the whole bridge, and the degree of construction difficulty caused by different closure conditions is different, the possibility of construction error is also different, and the accumulation of errors will be very different The construction of the closure is a difficult point in the construction of the whole bridge, and the degree of construction difficulty caused by different closure conditions is different, the possibility of construction error is also different, and the accumulation of errors will be very different [9].The closing stage is the most unstable stage in bridge construction, and the lack of grasp of each key section and process will lead to the failure of bridge closure or the construction quality is difficult to meet the design and specification requirements [10, 11]. Due to the long construction period of the long-linked long-span continuous beam bridge, the closing sequence is directly related to the organization and design of each construction process, which has a great impact on the arrangement of the construction period and cost control [12–14]. Through the study of the completed continuous beam bridges, it can be found that after many years of operation, the parts of the bridge with more diseases are in the middle of the span and the expansion joints, which are inseparable from the closure in the design and construction [15–17]. Therefore, it is the focus of the construction control work of long-linked continuous beam bridge to calculate and analyze the possible closure sequence, select a reasonable scheme or optimize the original scheme, and combine the accurate and effective closure control technology.

In this paper, four feasible closing schemes are proposed for engineering examples, and the working conditions, cumulative vertical displacement, lower edge stress on the section and horizontal displacement of the support are compared and analyzed under different closing sequence schemes. The optimization technology and construction control technology of the closing sequence can be used to solve the key problems in the construction control of the closure of the long-connected continuous beam bridge.

2. Project overview

A bridge is a continuous box girder with a 13-span variable cross-section, and the span layout is 59.7 m +11 × 100 m + 59.7 m. The superstructure adopts a single-box, single-chamber variable-section prestressed continuous box girder. The pier is a solid pier, wherein the 56th pier, the 69th pier are the transitional piers, and the junction with the cushion cap is provided with an icebreaker body, and the pier cap size is 1060 cm × 360 cm, and the pier body size

is 600 cm ×300 cm. The foundation is made of bored piles with a diameter of 180 cm. The purpose of designing the bridge as an ultra-long connection is two aspects, one is to increase the driving comfort and reduce the number of expansion joints. On the other hand, the annual temperature difference in this area is not large, and the expansion of the beam end is not large.

The beam height at the pier is 6.09 m, the middle span and the beam end beam height is 2.59 m, and the beam height is changed according to 1.6 parabolas in the range from block 0 to 49 m in the middle of the span. The top width of the box girder is 12 m, the width of the bottom plate is 6.0 m, and the cantilevered length of the wing plate is 3.0 m. The edge of the flange is 18 cm thick, and the flange support is 60 cm thick. Block 0 is 12 m long, Block 1~2 is 3.5 m long, Block 3~11 is 4 m long; the middle span closure section is 2 m long, and the side span closure section is 2 m long. The elevation and cross-sectional view of the bridge are shown in Fig. 1 and Fig. 2.

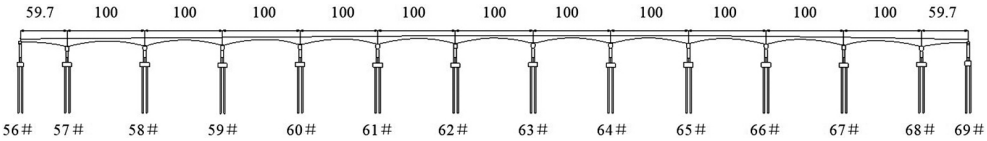

Fig. 1. Bridge elevation (unit: m)

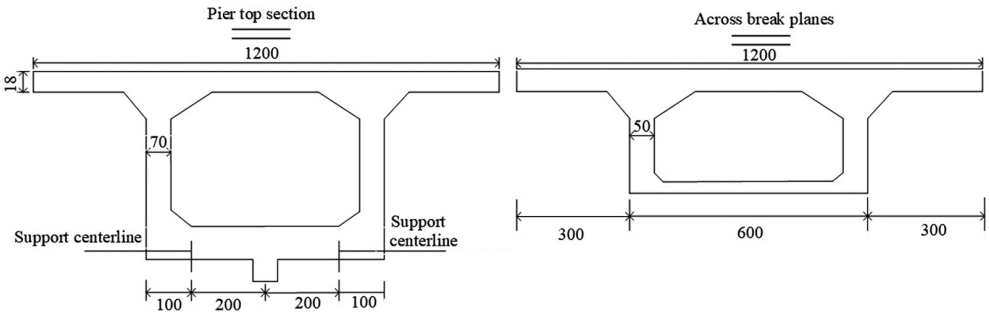

Fig. 2. Cross-sectional view of the bridge (unit: cm)

3. The bridge used for the closure of the dragon sequential scheme

The span of the continuous beam bridge is 59.7 m + 11 × 100 m + 59.7 m, which belongs to the long-linked long-span continuous beam bridge. According to the introduction of the previous section, several reasonable closure schemes are proposed mainly from the aspects of structural stress and construction period, and the more advantageous closing sequence is selected to achieve the purpose of optimization by comparing with the design scheme. There are four types of closure schemes that can be used for this bridge, as shown in Table 1.

The closing control principle of the long continuous beam bridge is that the cumulative deformation in the construction stage is minimum, and the stress change of the main beam in the closing process is minimum.

Table 1. Long-linked continuous beam bridge closure scheme

Scheme	Closure conditions			
	1	2	3	4
1	Second, fourth, sixth, eighth, tenth, and twelfth spans	Third, fifth, ninth, and eleventh spans	The first and thirteenth spans	Seventh span
2	Second, fourth, sixth, eighth, tenth, and twelfth spans	First, fifth, ninth, thirteenth span	Third, eleventh span	Seventh span
3	First, third, fifth, ninth, eleventh, thirteenth span	Second, sixth, eighth, and twelfth spans	Fourth, tenth span	Seventh span
4	First, third, fifth, seventh, ninth, eleventh, thirteenth span	Second, sixth, eighth, and twelfth spans	Fourth span	Tenth span

4. Calculation and analysis of different program processes

4.1. Option 1: Calculation and analysis

The first scheme is the original design scheme, which is the way to first close the dragon and then close the dragon.

Closure condition 1: the second, fourth, sixth, eighth, tenth, and twelfth crosses the first closure, forming 6 “T” structures, and lifting the temporary consolidation of 58#, 60#, 61#, 62#, 64#, 65#, and 67# piers.

Closure condition 2: the third, fifth, ninth and eleventh spans of closure, connect the formed “T” structure left and right into a whole, and lift the temporary consolidation of 59# and 66# piers.

Closure condition three: the first and thirteenth spans of the closure of the dragon, the overall side span closure that has been formed, the closure of the left and right halves of the bridge, and the temporary consolidation of the 57 # and 68 # piers will be lifted.

Closure condition four: the seventh span of the closure, the whole bridge closure, and the temporary consolidation of the 63# pier is lifted.

(1) Control the calculation of the vertical displacement of the cross-section

Through calculation, the maximum vertical displacement change point in the closing stage is near the mid-span cross-section, and the half-bridge is specially selected to explain due to the long length of the whole bridge (the vertical displacement and stress analysis of the subsequent schemes are analyzed by the half-bridge data, and no special description is not specified).

In scheme 1, the vertical displacement generated by the first closing condition is the largest, and the maximum displacement is –147.6 mm of the middle section of the seventh span, and the displacement of the break surface of each span under the second closing condition is relatively uniform, and the first and second working conditions form a "T" structure and connect the formed "T" structure left and right to form a whole, so the deformation curve is also a regular wavy shape.

(2) Calculation of stress at the upper and lower edges of the control section

Through the calculation and other engineering examples, it is verified that the extreme stress points of the upper and lower edges of the main girder in the construction stage of closure are near the pier, *L*/4, and the middle span section, so these cross-sections are also selected as the stress control cross-sections of the main girder in the construction control.The stress changes on the control sections and lower edges of each control section under the closing conditions of the half-bridge are shown in Fig. 3 and Fig. 4.

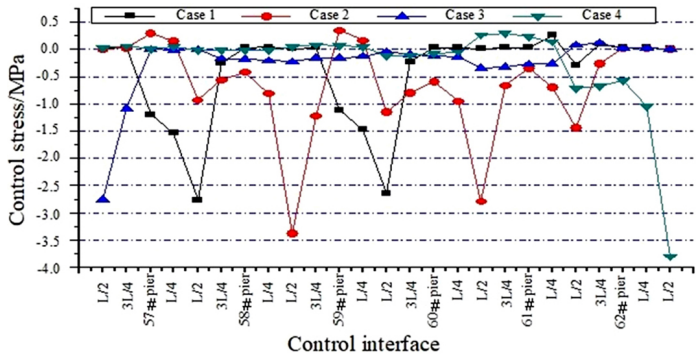

Fig. 3. Variation of stress at the upper edge of the control section under each working condition

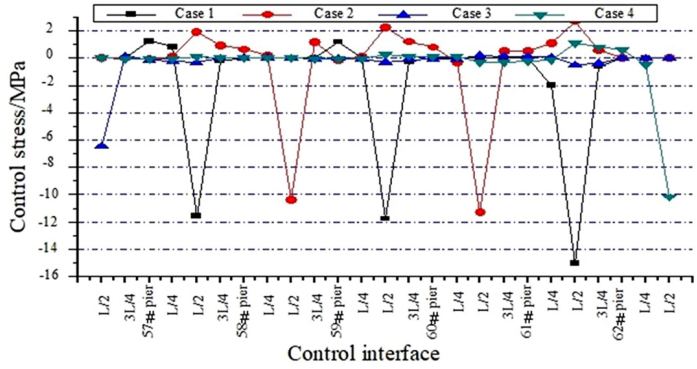

Fig. 4. Stress variation diagram of the lower edge of the control section under each working condition

It can be seen from Fig. 3 and Fig. 4 that the maximum change of stress at the upper edge of the main beam in the process of scheme 1 closing is –3.8 MPa in the middle span of the closing dragon, and this part of the stress should be paid attention to in the construction

control. The stress of the lower edge changes greatly, and the largest change occurs in the middle section of the sixth span of case 1 –15.06 MPa, and the cross-sectional stress is also the maximum value of the scheme –16.31 MPa, affected by the fixed support of the 62# pier, the stress of the upper edge of the span after the closure of the dragon does not change much, and the compressive stress of the section is mainly borne by the lower edge.

4.2. Option 2: Calculation and analysis

Scheme 2 optimizes the original design scheme, the first and thirteenth spans are closed in the second working condition, and the third and eleventh spans are combined in the third and eleventh spans under the working condition, but the temporary consolidation and release status remains unchanged.

(1) Control the calculation of the vertical displacement of the cross-section.

The maximum vertical displacement change also appears in the seventh span in case 1, which is –147.46 mm, but the vertical displacement change of the other working conditions is smaller than that of scheme 1, indicating that the vertical displacement change of the main beam is also quite different if the closing sequence is changed, but the temporary consolidation is not changed.

The upper and lower edges of the main beam do not appear tensile stress in the closing conditions of scheme 2, and the compressive stresses do not exceed the limit, and the stress changes on the control sections and lower edges of the half-bridge under the closing conditions are shown in Fig. 5 and Fig. 6.

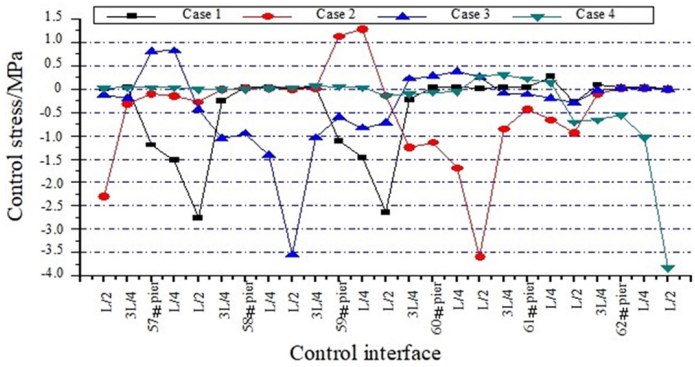

Fig. 5. Variation of stress at the upper edge of the control section under each working condition

It can be seen from Fig. 5 and Fig. 6 that the stress change law of the upper and lower edges of the main beam in the process of scheme 2 is like that of scheme 1. The maximum change of stress at the upper edge is –3.82 MPa in the middle span of the closing dragon. The cross-section of the sixth span in case 1 is –15.06 MPa, and the cross-sectional stress is also the maximum value of –15.22 MPa in this scheme.

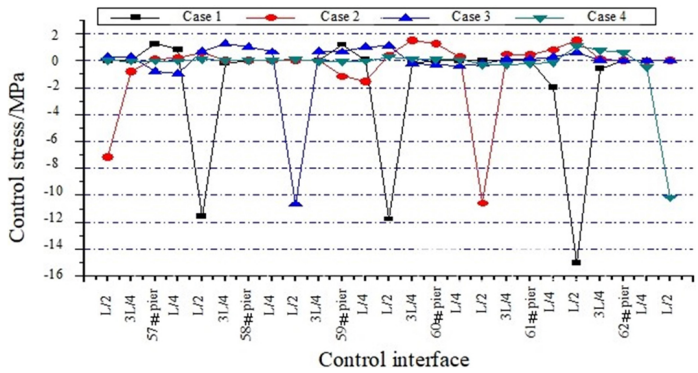

Fig. 6. Stress variation diagram of the lower edge of the control section under each working condition

4.3. Option 3: Calculation and analysis

Scheme 3 is the same as the way of first combining the small dragon and then the big dragon, but the odd number of dragons is crossed first.

Closure condition 1: the first, third, fifth, ninth, eleventh, and thirteenth cross the first closure, forming 6 "T" structures, and lifting the temporary consolidation of 58#, 60#, 65#, and 66# piers.

Closure condition 2: the second, sixth, eighth, and twelfth spans of Helong, and the temporary consolidation of 57#, 61#, 62#, 64#, and 68# piers is lifted.

Closure condition 3: the fourth and tenth spans of the closure, the left and right halves of the bridge are closed, and the temporary consolidation of the 59# and 67# piers is lifted.

Closure condition 4: the seventh span of the closure, the whole bridge closure, and the temporary consolidation of the 63# pier is lifted.

(1) Control the calculation of the vertical displacement of the cross-section

The maximum value of vertical displacement change occurs in the seventh span caused by the sixth span of the closing dragon in case 2, which is –63.88 mm, and it can be seen that the change of each control section in the first working condition of the closing dragon is significantly lower than that of the first two schemes, and the change values of the third and fourth working conditions are greater than those of the first two schemes, that is, the vertical displacement change of each working condition under this scheme is more uniform.

(2) Control the cross-section stress calculation

There is no tensile stress on the upper and lower edges of the beam in the closing conditions of scheme 3, and the compressive stresses do not exceed the limit, and the stress changes on the control sections and lower edges of the half-bridge under the closing conditions are shown in Fig. 7 and Fig. 8.

It can be seen from Fig. 7 and Fig. 8 that the maximum stress change of the upper edge of the main beam in the process of the third parallel scheme is slightly larger than that of the first two schemes, and the maximum value is –3.99 MPa in the middle span of the second span of the closing dragon. The stress change of the lower edge is smaller than that of the first two

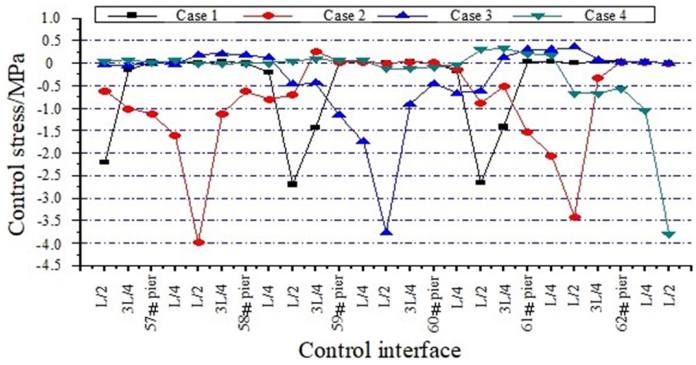

Fig. 7. Variation of stress at the upper edge of the control section under each working condition

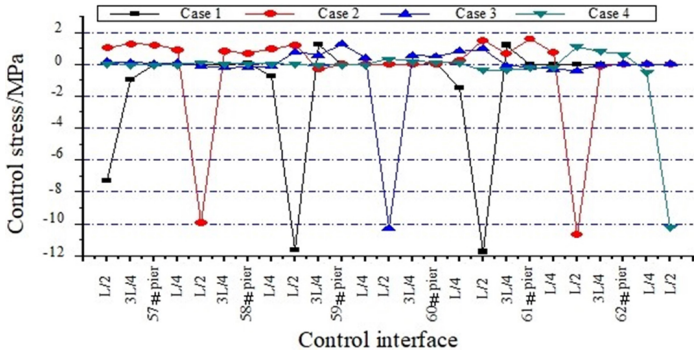

Fig. 8. Stress variation diagram of the lower edge of the control section under each working condition

schemes, and the maximum value occurs at –11.76 MPa in the middle span of the third span of the first case, and the stress value is –12.60 MPa. In general, the stress changes generated by the working conditions of scheme 3 are better.

4.4. Scheme 4: Calculation and analysis

Closure condition 1: the first, third, fifth, seventh, ninth, eleventh, and thirteenth cross the first closing, and lift the temporary consolidation of 58#, 60#, 62#, 63#, 65#, and 67# piers.

Closure condition 2: the second, sixth, eighth, and twelfth spans of closure, and the temporary consolidation of 57#, 61#, 64#, and 68# piers is lifted.

Closure condition 3: closure fourth span, release 59# pier temporary consolidation.

Closure condition 4: the tenth span of the closure, the whole bridge closure, and the temporary consolidation of the 66# pier is lifted.

(1) Control the calculation of the vertical displacement of the cross-section

The vertical displacement changes value of each mid-span control section is shown in Fig. 9.

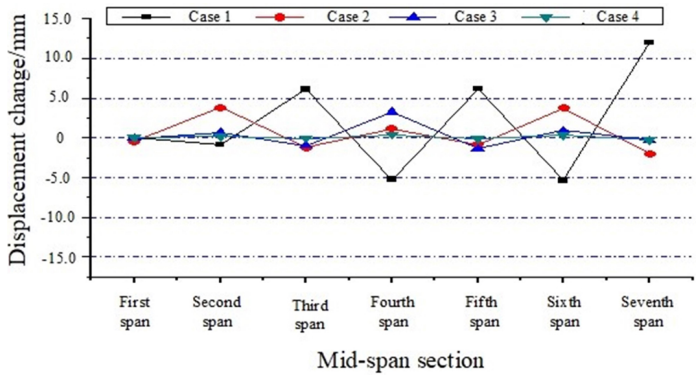

Fig. 9. Vertical displacement change diagram in the span of each working condition

It can be seen from Fig. 9 that the maximum value of vertical displacement change is similar to other schemes and appears in the seventh span in case 1, which is 119.26 mm, but the difference is that the reverse camber value is caused by the tensioning of the prestressed beam of the closure in the seventh span of case 1 closure, and compared with the first three schemes, the vertical displacement change value of this scheme is in the middle, and the change is basically completed in the first three working conditions.

(2) Control the cross-section stress calculation

There is no tensile stress at the upper and lower edges of the main beam in the closing conditions of scheme four, and the compressive stresses are not exceeded, and the stress changes on the control sections and lower edges of the half-bridge under the closing conditions are shown in Fig. 10 and Fig. 11.

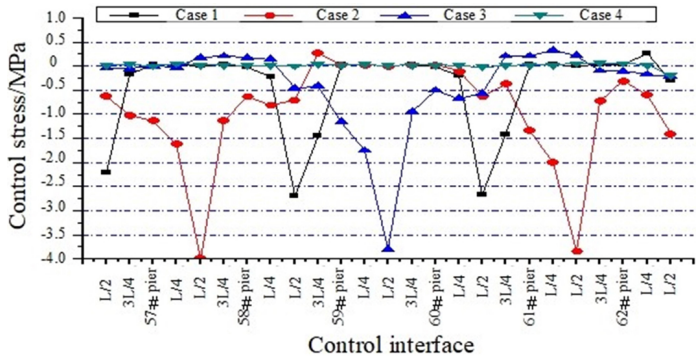

Fig. 10. Variation of stress at the upper edge of the control section under each working condition

It can be seen from Fig. 10 and Fig. 11 that the stress trend of the upper and lower edges of the main beam in the process of the four-step scheme is also like that of the other three schemes. It shows that there is little difference in the influence of displacement and internal force between the comprehensive application method of small and large dragons and the method of small dragon and then large dragon, and the purpose of optimization can also be

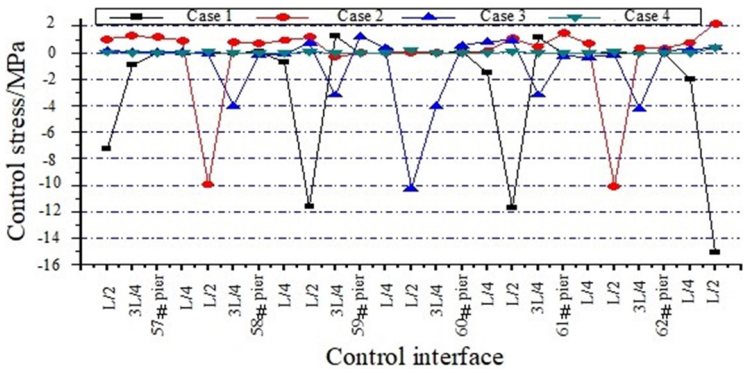

Fig. 11. Stress variation diagram of the lower edge of the control section under each working condition

achieved by changing the method of dragon closure. The maximum value of the stress change at the upper edge of scheme 4 is –3.99 MPa in the middle section of the second span in case 2, and the stress change at the lower edge is larger, and the maximum value appears in the middle section of the seventh span in case 1 at –15.06 MPa, and the stress at the lower edge of the section is –15.33 MPa. The magnitude of the stress change is also in the middle of the four schemes, which is better than scheme 1 and 2, but worse than scheme 3.

5. Comparative analysis of different schemes

5.1. Comparison of vertical displacements

The maximum vertical displacement of each scheme in each closing case appears in the middle section of the seventh span, and the maximum value of each scheme is shown in Table 2.

Table 2. Maximum vertical displacement in the middle span of each scheme and working condition (mm)

Project	Option 1	Option 2	Option 3	Option 4
Maximum	–147.60	–147.46	–63.88	119.26

After the closure of each dragon scheme, the cumulative vertical displacement of each span in the bridge formation stage is shown in Fig. 12. The cumulative vertical displacement of the super-long joint large-span prestressed continuous girder bridge in the construction stage is relatively large, and the cumulative maximum can reach –117.5 mm. The deformation curve is basically symmetrical at the center of the bridge, reaching a maximum value at the front end of each span. However, with the different closure sequence schemes, although the position of the extreme point of the vertical displacement of the main beam in each working condition is basically the same, the cumulative maximum value point of the whole bridge appears in different spans, and the alignment of the bridge also changes.

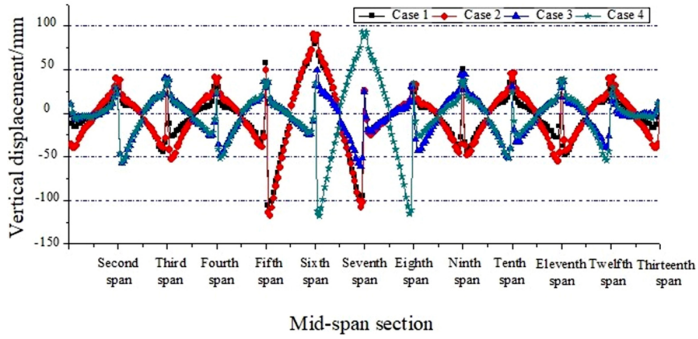

Fig. 12. Cumulative vertical displacement of each scheme into a bridge

The maximum vertical displacement of scheme 1 and 2 in the process of closing the dragon under each working condition can reach –147.60 mm, and the actual value is often greater than the theoretical calculated value due to the more system conversion and other influencing factors in the construction process, which is unfavorable for reducing the construction error and realizing that the height difference between the two ends of the closing section is not more than 20 mm. Option three is the smallest, while option four is in the middle.

Secondly, the cumulative vertical displacement scheme of the bridge is –109.7 mm, the second scheme is –116.9 mm, the fourth scheme is –117.5 mm, and the third scheme is only –61.2 mm.

5.2. Stress comparison

The maximum stress changes at the upper and lower edges of each scheme appear in the mid-span cross-section, and the maximum changes of each scheme are shown in Table 3.

Table 3. Maximum changes in the upper and lower and edge stresses of each scheme and under each working condition (MPa)

Project	Option 1	Option 2	Option 3	Option 4
Upper edge maximum	–10.00	–10.60	–10.40	–10.40
Lower edge maximum	–16.31	–15.22	–11.76	–15.33

After closing according to each scheme, the cumulative stress values of the upper and lower edges of the main girder of the whole bridge in the bridge formation stage are shown in Fig. 13 and Fig. 14.

It can be seen from Fig. 13 and Fig. 14 that the stress at the upper and lower edges of the main beam is compressive stress under the four closing schemes (the symbol stipulates: the tensile stress is positive, and the compressive stress is negative), and the position of the extreme point of the curve is basically the same and does not change with the difference of the closing order.

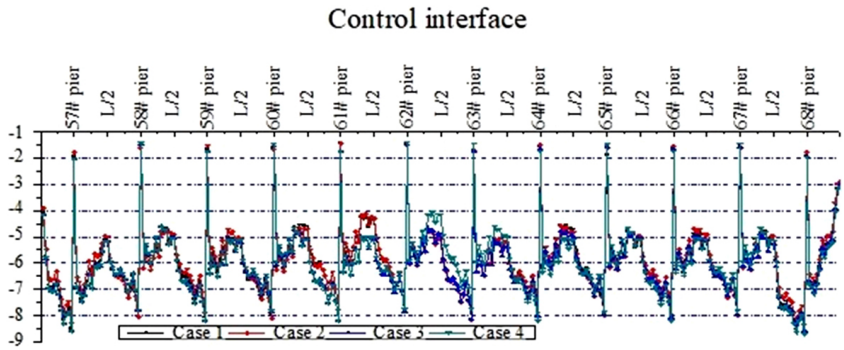

Fig. 13. Stress diagram of the upper edge of the main girder of each scheme

In each closing case, the middle span where the maximum value of each stress is located is different due to the different closing sequence, and the maximum value of stress change and the cumulative maximum value of stress at the upper edge are basically unchanged, but the maximum value of stress change and the cumulative maximum value of lower edge are quite different: the maximum value is –15.06 MPa of scheme 1, 2 and 4, and the minimum value is –11.76 MPa of scheme 3, the maximum value of cumulative maximum value is –16.31 MPa of scheme 1, and the minimum value is –11.76 MPa of scheme 3.

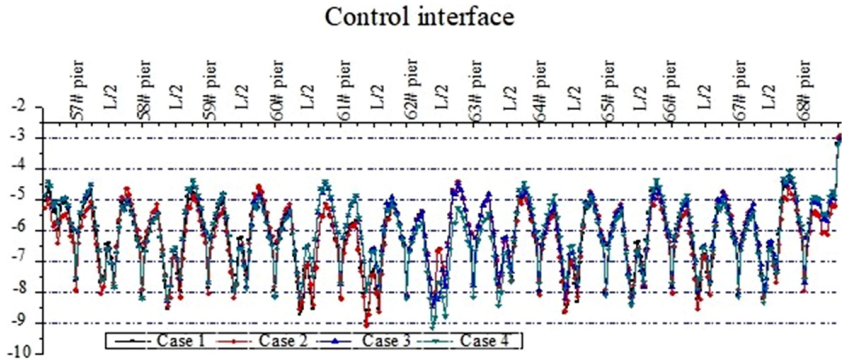

Fig. 14. Stress diagram of the lower edge of the main girder of each scheme

The minimum value difference is 0.4 MPa to the bridge stage, the upper edge of the main beam obtains the maximum stress value at the front section of each span 0# block and obtains the minimum value at the top of each pier, and the stress in the single span is basically symmetrically distributed, and the small value is obtained in the middle span section. The maximum value occurs at the front section of the secondary side span 0# block, and the minimum value is at the top section of the side pier. The maximum stress values of the upper edge of each scheme are –8.57 MPa, –8.33 MPa, –8.59 MPa, –8.67 MPa, and the minimum stress values are –1.47 MPa, –1.44 MPa, –1.46 MPa, and –1.45 MPa.

5.3. Comparison of horizontal displacements of supports

Under the action of factors such as system conversion, prestressed beam tension, temperature change, concrete shrinkage and creep, the movable bearing and the beam end will produce a large longitudinal displacement, and the longitudinal offset between the upper seat plate of the pier bearing and the theoretical center line of the support needs to be preset, to avoid the eccentric stress of the bearing. The longitudinal displacement of the support under the different closing schemes is shown in Fig. 15.

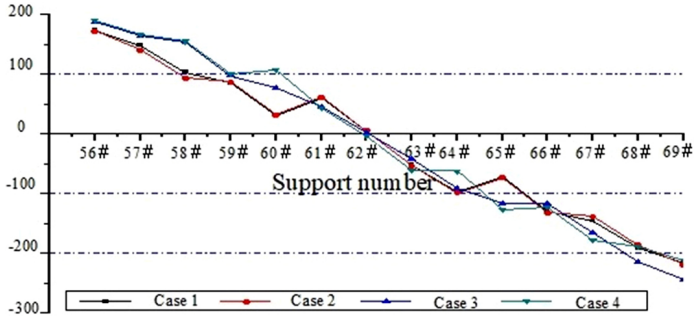

Fig. 15. Longitudinal displacement diagram of each scheme support

It can be seen from Fig. 18 that under different closure schemes, the longitudinal displacement of the support is basically the same, and the symmetrical change along the fixed support (arranged at pier 62) changes, and the magnitude increases with the increase of the distance away from the fixed support. Under the four schemes, the side pier bearing changes the most, and the maximum value reaches –243.4 mm. The maximum longitudinal displacement difference of each pier support appears in 60# pier support, which is 75.95 mm. The large longitudinal deformation will lead to a large pre-deviation setting of the support and affect the selection and laying of the expansion joint at the beam end. Therefore, scheme 2, which has a small longitudinal displacement at each support and beam end, has advantages among several schemes, but at the same time, it is also found that schemes 3 and 4 have better overall distribution, and the support pre-deviation setting is more convenient.

6. Choice of scheme

6.1. Achievements of the whole bridge construction control

The elevation error of the key section of the whole bridge is shown in Fig. 16.

When the bridge is measured, it is found that after the construction control of the bridge, the elevation of the whole bridge is within the error control range, which meets the requirements of the specification and design, and the elevation of the middle of the bridge section is slightly larger than the design value, and the maximum value is 22 mm, which is beneficial to the deflection of the main beam in the later stage.

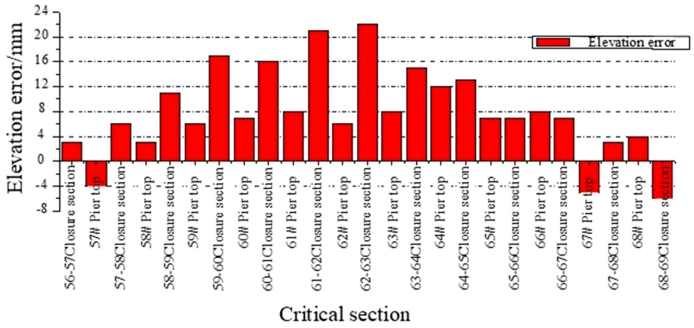

Fig. 16. Elevation error diagram of key sections in the bridge formation stage

The stress values of each stress control section are not exceeded in each construction stage, and the stress at the upper and lower edges in the bridge forming stage is shown in Fig. 17 and Fig. 18.

It can be seen from Fig. 17 and Fig. 18 that the measured stress in the bridge formation stage is basically consistent with the theoretical calculated value, and the stress distribution is relatively uniform, indicating that the selected scheme has a reasonable sequence of three dragons, and the construction control measures are appropriate, and the bridge construction state meets the design and specification requirements. 3

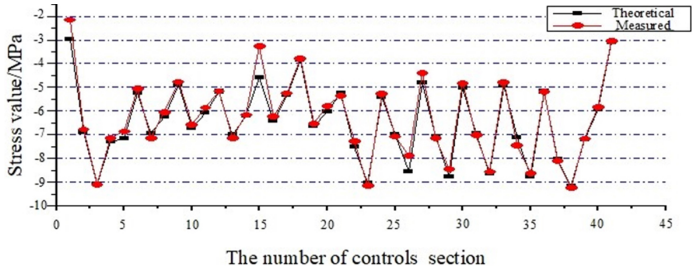

Fig. 17. Stress diagram of the upper edge of the control section during the bridge formation stage

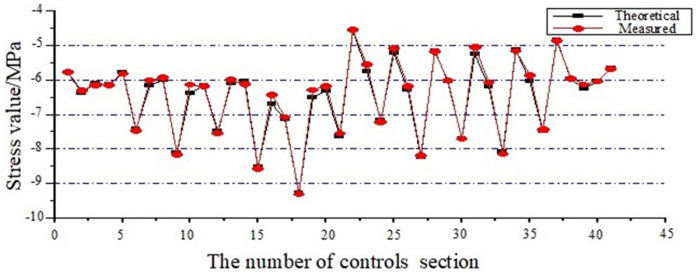

Fig. 18. Stress diagram of the lower edge of the control section during the bridge formation stage

7. Conclusions

Based on the established finite element model, combined with the common long-connected continuous beam bridge closure sequence scheme, four feasible schemes are proposed for this engineering example, three of which are optimization schemes, taking the deformation and internal force of the main beam as the control elements, the vertical displacement and the stress change on the lower edge of the section generated by each closing condition under different closing sequence schemes are calculated and analyzed, and the cumulative vertical displacement, the stress on the lower edge of the section and the horizontal displacement of the support under each scheme are compared and analyzed.

(1) It is necessary to carry out optimization research, and the reasonable scheme is not the only one, and various factors should be considered comprehensively when formulating the construction organization plan, and the schemes should be comprehensively compared, and the actual situation should be considered from a technical point of view.

(2) The construction control of the closure stage is studied, and the verification results of the bridge construction control show that the optimization technology and construction control technology of the closure sequence are used in this paper, which solves the key problems in the construction control of the closure of long-link continuous beam bridges and can provide reference and basis for the construction control of the same type of bridge.

(3) The maximum value occurs at the front section of the secondary side span 0# block, and the minimum value is at the top section of the side pier. The maximum stress values of the upper edge of each scheme are –8.57 MPa, –8.33 MPa, –8.59 MPa, –8.67 MPa, and the minimum stress values are –1.47 MPa, –1.44 MPa, –1.46 MPa, and –1.45 MPa.

(4) The cumulative vertical displacement scheme of the bridge is –109.7 mm, the second scheme is -116.9 mm, the fourth scheme is –117.5 mm, and the third scheme is only –61.2 mm.

References

[1] H. Zhiguo, L. Wentao, H. Salehi, et al., “Integrated structural health monitoring in bridge engineering”, *Automation in Construction*, vol. 136, art. no. 104168, 2022, doi: 10.1016/j.autcon.2022.104168.

[2] Z. Jiang, X. Shen, M. H. Ibrahimkhil, et al., “Scan-VS-BIM for real-time progress monitoring of bridge construction project”, *ISPRS Annals of the Photogrammetry, Remote Sensing and Spatial Information Sciences*, vol. 10, pp. 97–104, 2022, doi: 10.5194/isprs-annals-X-4-W3-2022-97-2022.

[3] T. Jiahao, L. Sang, W. Xinming, et al., “Crane lifting optimization and construction monitoring in steel bridge construction project based on BIM and UAV”, *Advances in Civil Engineering*, vol. 2021 pp. 1–15, 2021, doi: 10.1155/2021/5512229.

[4] D. Inaudi, A. Ruefenacht, et al., “Monitoring of a concrete arch bridge during construction”, *Smart Structures and Materials*, vol. 4696, 2002, doi: 10.1117/12.472550.

[5] P. Omenzetter, J.M.W. Brownjohn, and P. Moyo, “Identification of unusual events in multi-channel bridge monitoring data”, *Mechanical Systems and Signal Processing*, vol. 18, no. 2, pp. 409–430, 2004, doi: 10.1016/S0888-3270(03)00040-2.

[6] L.J. Butler, L. Weiwei, et al., “Monitoring, modeling, and assessment of a self-sensing railway bridge during construction”, *Journal of Bridge Engineering*, vol. 23, no. 10, 2018, doi: 10.1061/(ASCE)BE.1943-5592.0001288.

[7] P. Omenzetter and J.M.W. Brownjohn, “Application of time series analysis for bridge monitoring”, *Smart Materials and Structures*, vol. 15, no. 1, art. no. 129, 2006, doi: 10.1088/0964-1726/15/1/041.

[8] B. Yong, J. Huan, and K. Seonghoon, "Measuring bridge construction efficiency using the wireless real-time video monitoring system", *Journal of Management in Engineering*, vol. 28, no. 2, pp. 120–126, 2012, doi: 10.1061/(ASCE)ME.1943-5479.0000061.

[9] L. Yungbin, P. Chinliang, et al., "Online monitoring of highway bridge construction using fiber Bragg grating sensors", *Smart Materials and Structures*, vol. 14, no. 5, art. no. 1075, 2005, doi: 10.1088/0964-1726/14/5/046.

[10] F. Meizhen, L. Yuxiong, F. Qingsong, et al., "Research on the application of multi-source data analysis for bridge safety monitoring in the reconstruction and demolition process", *Buildings*, vol. 12, no. 8, art. no. 1195, 2022, doi: 10.3390/buildings12081195.

[11] W. Baolin, "Using fiber-reinforced polymer (FRP) composites in bridge construction and monitoring their performance: An overview", in *Advanced composites in bridge construction and repair*. Elsevier, 2014, pp. 3–29, doi: 10.1533/9780857097019.1.3.

[12] S. Helder, J. Bento, and J. Figueiras, "Construction assessment and long-term prediction of prestressed concrete bridges based on monitoring data", *Engineering Structures*, vol. 52, pp. 26–37, 2013, doi: 10.1016/j.engstruct.2013.02.003.

[13] L. Fangyuan, W. Peifeng, and Y. Xinfei, "Analysis and monitoring on jacking construction of continuous box girder bridge", *Computers and Concrete*, vol. 16, no. 1, pp. 49–65, 2015, doi: 10.12989/cac.2015.16.1.049.

[14] L. Hui, O. Jinping, et al., "Structural health monitoring system for the Shandong Binzhou Yellow River highway bridge", *Computer-Aided Civil and Infrastructure Engineering*, vol. 21, no. 4, pp. 306–317, 2006, doi: 10.1111/j.1467-8667.2006.00437.x.

[15] A. Scianna, G.F. Gaglio, and M.L. Guardia, "Structure monitoring with BIM and IoT: The case study of a bridge beam model", *ISPRS International Journal of Geo-Information*, vol. 11, no. 3, 2022, doi: 10.3390/ijgi11030173.

[16] Z. Qiwei and Z. Yan, "Investigation of the applicability of current bridge health monitoring technology", *Structure and Infrastructure Engineering*, vol. 3, no. 2, pp. 159–168, 2007, doi: 10.1080/15732470600590762.

[17] Z. Guangdong, Y. Tinghua, et al., "Standardization construction and development trend of bridge health monitoring systems in China", *Advances in Bridge Engineering*, vol. 1, pp. 1–18, 2020, doi: 10.1186/s43251-020-00016-5.

Received: 2024-06-11, Revised: 2024-08-14